

2  
Comb-901105--87

UCRL- JC-103725  
PREPRINT

UCRL-JC--103725

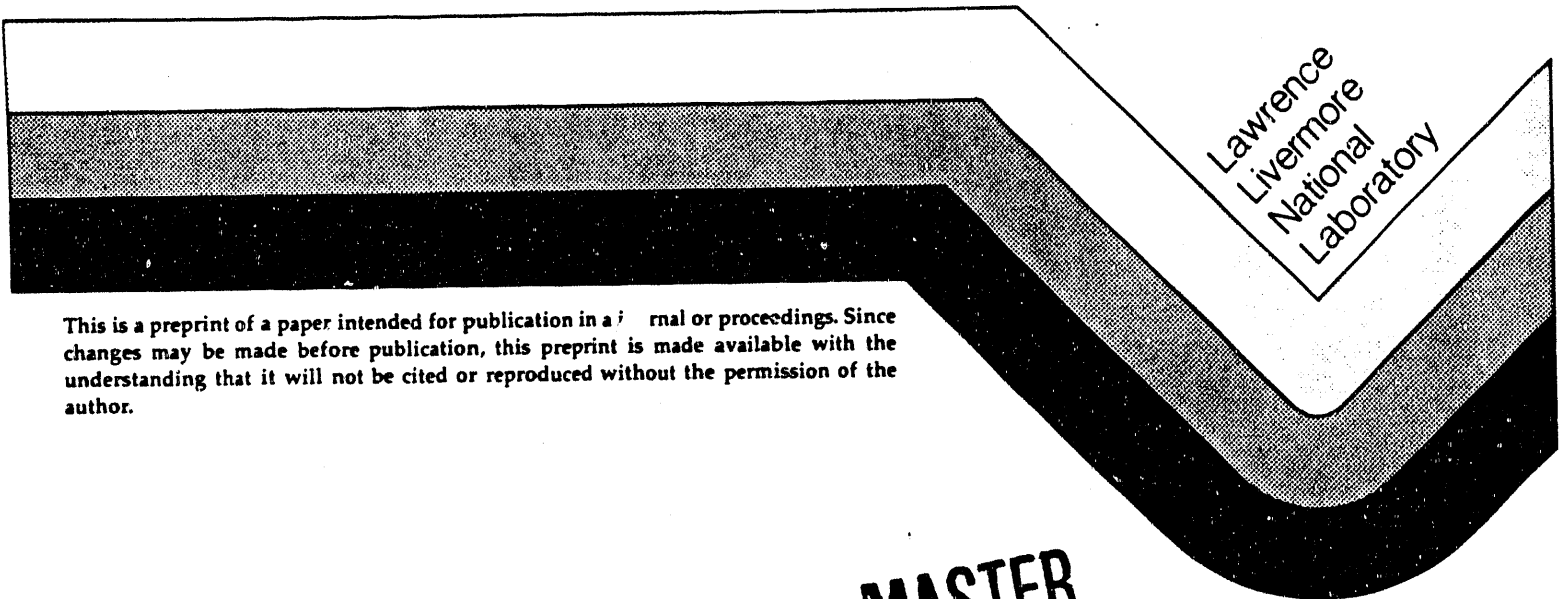
DE91 007254

Photoelectron Diffraction of Magnetic  
Ultrathin Films: Fe/Cu(001)

J. G. Tobin  
M. K. Wagner  
X.-Q. Guo  
S. Y. tong

This paper was prepared for submittal to  
MRS Fall Meeting  
Boston, MA  
Nov. 25 - Dec. 1, 1990

Jan. 3, 1991



Lawrence  
Livermore  
National  
Laboratory

This is a preprint of a paper intended for publication in a journal or proceedings. Since changes may be made before publication, this preprint is made available with the understanding that it will not be cited or reproduced without the permission of the author.

**MASTER**

*JMP*  
DISTRIBUTION OF THIS DOCUMENT IS UNLIMITED

#### DISCLAIMER

This document was prepared as an account of work sponsored by an agency of the United States Government. Neither the United States Government nor the University of California nor any of their employees, makes any warranty, express or implied, or assumes any legal liability or responsibility for the accuracy, completeness, or usefulness of any information, apparatus, product, or process disclosed, or represents that its use would not infringe privately owned rights. Reference herein to any specific commercial products, process, or service by trade name, trademark, manufacturer, or otherwise, does not necessarily constitute or imply its endorsement, recommendation, or favoring by the United States Government or the University of California. The views and opinions of authors expressed herein do not necessarily state or reflect those of the United States Government or the University of California, and shall not be used for advertising or product endorsement purposes.

PHOTOELECTRON DIFFRACTION OF MAGNETIC ULTRATHIN FILMS:  
Fe/Cu(001)

J. G. TOBIN,\* M. K. WAGNER,\*\* X.-Q. GUO\*\*\* AND S. Y. TONG\*\*\*

\*Lawrence Livermore National Laboratory, Livermore, California 94550

\*\*Dept. of Chemistry, University of Wisconsin, Madison, WI 53706

\*\*\*Dept. of Physics, University of Wisconsin, Milwaukee, WI 53211

ABSTRACT

The preliminary results of an ongoing investigation of Fe/Cu(001) are presented here. Energy dependent photoelectron diffraction, including the spin-dependent variant using the multiplet split Fe 3s state, is being used to investigate the nanoscale structures formed by near-monolayer deposits of Fe onto Cu(001). Core-level photoemission from the Fe3p and Fe3s states has been generated using synchrotron radiation as the tunable excitation source. Tentatively, a comparison of the experimental Fe3p cross section measurements with multiple scattering calculations indicates that the Fe is in a fourfold hollow site with a spacing of 3.6Å between it and the atom directly beneath it, in the third layer. This is consistent with an FCC structure. The possibility of utilizing spin-dependent photoelectron diffraction to investigate magnetic ultrathin films will be demonstrated, using our preliminary spectra of the multiplet-split Fe3s of near-monolayer Fe/Cu(001).

INTRODUCTION

Photoelectron diffraction, both non-spin and spin-dependent, is being used to investigate the magnetic ultrathin film system, Fe/Cu(001). Fe/Cu(001) is the prototypical model system of magnetic ultrathin films, yet remains the subject of considerable controversy. For example, a theoretical study[1] predicts a large magnetic moment at a coverage of one monolayer, assuming perfect pseudomorphic growth. Nevertheless, surface magneto optic Kerr effect (SMOKE) measurements indicate an absence of such a magnetic moment, leading to the hypothesis of surface alloying [2]. Photoelectron diffraction has been shown to be a powerful probe of atomic geometric structure, particularly surface alloying [3]. We are performing a photoelectron diffraction study of Fe/Cu(001), using the Fe3p and Fe3s states and including a full, multiple scattering analysis. Moreover, a new variant, spin-dependent photoelectron diffraction[4] (SDPD) using the multiplet-split 3s state, will be discussed. SDPD promises to be a probe of both local geometric and magnetic structure, thus providing a nanoscale counterpart to SMOKE measurements.

DISCUSSION

Photoelectron diffraction is a probe that can be used to investigate the local (nanoscale,  $10^{-9}$  m) geometric structure of surfaces and interfaces and which may be adaptable to determining local magnetic structure as well. Photoelectron diffraction can be thought of as an angle-resolved surface-extended-x-ray-absorption-fine-structure (SEXAFS) measurement. In our experiments, photoelectrons are ejected from core levels and can be involved with diffraction events caused by scattering off of nearby neighbors (figure 1). From this, the local geometric structure can be determined to within  $\pm 0.05\text{\AA}$  [5]. Our experiments are performed at low kinetic energy in order to maximize surface sensitivity [3] and the manifestation of magnetic effects. Thus it is essential that all analysis be performed within the framework of multiple-scattering calculations. The simplifications of single-scattering theory [4,6] are not appropriate except at higher kinetic energies. Moreover, the potential importance of surface alloying in the Fe/Cu(001) system militates against an over-reliance on forward focussing measurements, [6,7,8] which is a powerful probe of stacked or buried layers but is unable to distinguish an overlayer from a surface alloy [3, 9]. Finally, Sinkovik and Fadley [4] have pointed out the possibility of utilizing the multiplet split 3s peaks as a source of spin polarized electrons in these experiments. Recent spin-polarized photoemission investigations [10,11] of the Fe3s peak of bulk Fe have confirmed that these two peaks are in fact spin up and spin down in magnetized samples. Thus, we are beginning to use this intrinsic spin resolution in the investigation of magnetic ultrathin films, specifically Fe/Cu(001). It is not unreasonable to expect an approximately 10% effect, as is observed in spin polarized secondary electron spectroscopy [12]. Of course, a fully spin-parameterized, multiple scattering theory must and is being developed also.

Presented at Symposium J of the 1990  
Fall Meeting of the Materials Research  
Society, Boston, MA, and submitted to  
Mat. Res. Soc. Symp. Proc.

Figure 1. This schematic illustrates the underlying cause of photoelectron diffraction, interference between the direct and scattered waves. The interference is dependent upon the details of the local geometry and the emission angles and kinetic energy of the outgoing electron. The kinetic energy is varied by scanning the photon energy,  $h\nu$ . The binding energy ( $B^F$ ), the work function ( $\phi$ ), and inner potential ( $V_0$ ) are constant for a given state and material system.

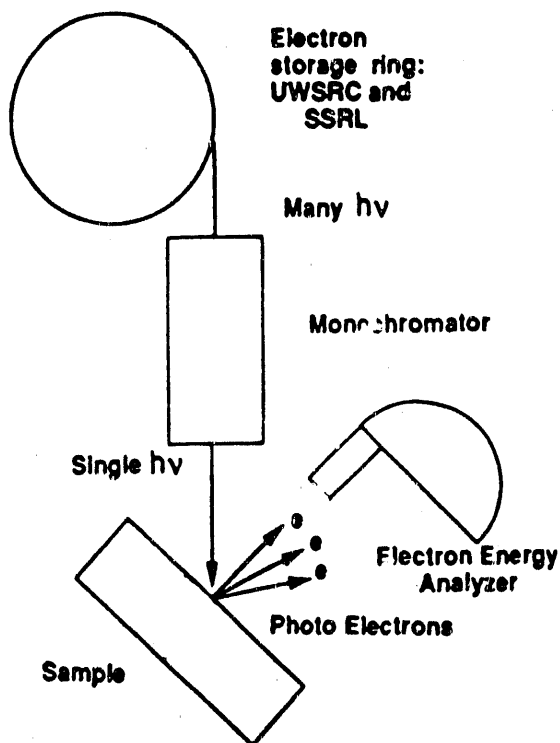
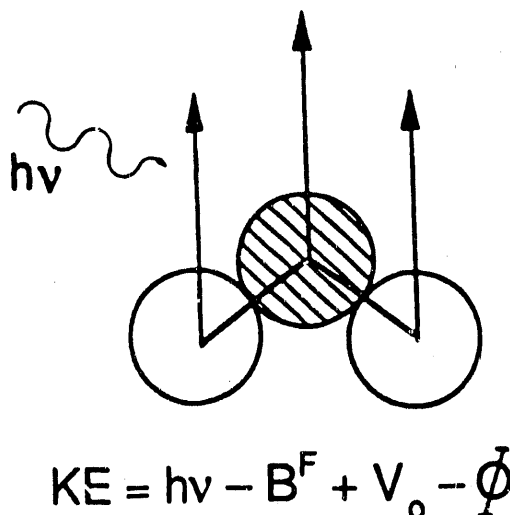


Figure 2. This figure shows schematically the experimental setup. A single energy ( $h\nu$ ) of electromagnetic radiation is selected from the broad continuum of synchrotron radiation using a monochromator. The photons cause the ejection of photoelectrons, which are then collected by the angle ( $\pm 3^\circ$ ) and energy resolving detector. The synchrotron radiation was provided by the University of Wisconsin Synchrotron Radiation Center (UWSRC) and the Stanford Synchrotron Radiation Laboratory (SSRL).

Several technical details should be discussed before moving on to the results. The variability of the kinetic energy is obtained via the tunability of synchrotron radiation, as shown in figures 1 and 2. Examples of the capabilities of the photoelectron spectrometer are published elsewhere [3,9]. All experiments and evaporations were performed under ultra-high vacuum conditions. Accurate coverage estimates are important to these studies. Low energy electron diffraction (LEED), Auger electron spectroscopy (figure 3), valence band photoemission (figure 4) and a thickness analysis using a quartz crystal microbalance were all used to monitor deposition levels. Fe was evaporated from an effusive-beam thermal source and the Cu(001) sample was at or near room-temperature during deposition and the photoelectron diffraction measurements. An "elbow" was observed in the plot of the Auger ratio of Fe intensity divided by Cu intensity (figure 3) and we have assigned a deposition value of the equivalent of a "monolayer", i.e.  $\theta = 1$  at this point, based upon internal consistencies in this and the other measurements. Nevertheless, this coverage estimate is limited by the following caveats: (1) The actual geometric structure is unknown and possibly is not an epitaxial overlayer; (2) the meaning and possibly even the existence of the "elbow" is in doubt [13,14]; (3) the coverage estimate is probably fairly precise (reproducible) but in absolute terms (accuracy) only good to within a factor of two. Our strategy is thus to do a series of coverages and look for consistencies in the scattering.

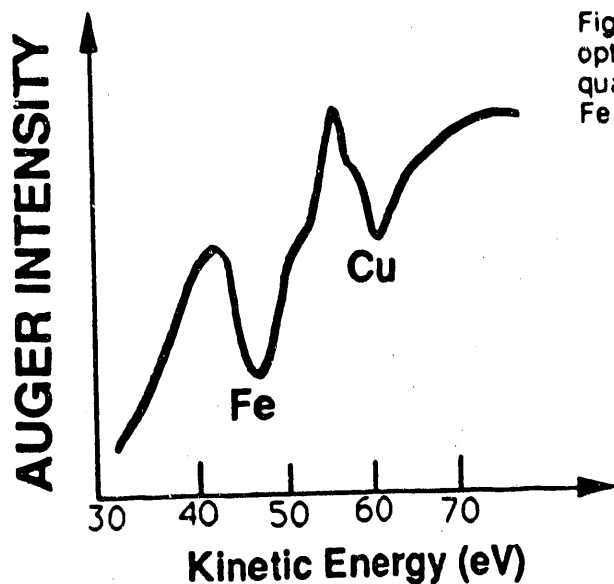
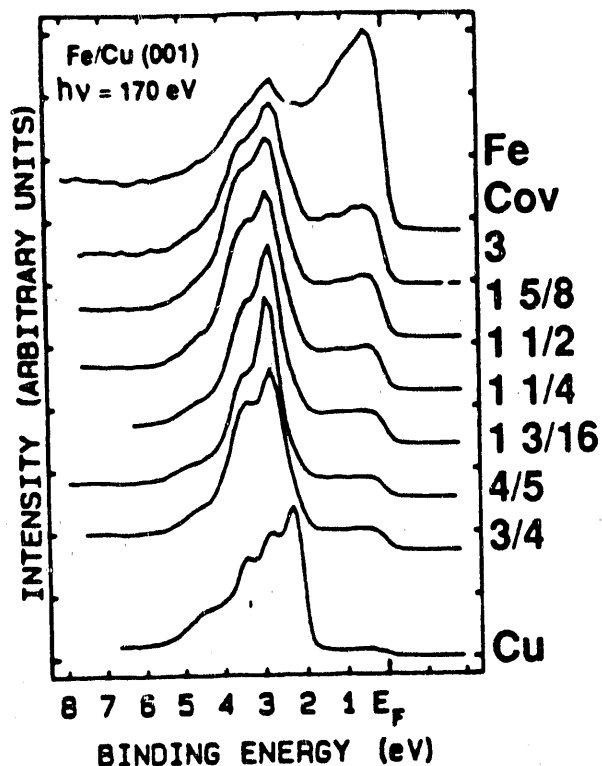


Figure 4. Normal emission photoemission of the valence bands is shown here, for a variety of coverages from zero (clean Cu(001)) to  $\Theta = 3$ . Note the attenuation of the Cu spectral structure at  $B^F = 2$  and the rise in the intensity at the Fermi edge, with increasing Fe coverage.

Figure 3. Auger electron spectroscopy, using LEED optics as a retarding field analyzer, have been used to quantify deposition via the effusive evaporator-source of Fe. Shown here is a spectrum at  $\Theta = 1$ .



The photoelectron diffraction experiment uses either the Fe3s or Fe3p levels as the internal and elementally specific source of electrons for the diffraction experiment. A simplified, atomistic view of the Fe electronic structure is shown in figure 5 and examples of photoelectron spectra of Fe/Cu(001) are presented in figure 6. The valence bands of the Fe will be strongly affected by neighboring atoms and this will include complications such as crystal field effects, spin-orbit splitting and delocalization. Nevertheless, it is reasonable to postulate some preferred alignment of spins in a magnetic system. It is the interaction of the remaining unbalanced spin in the Fe3s or Fe3p with the aligned 3d spins, after the photo-ionization, that causes the splitting of the Fe3s peak and asymmetry in the Fe3p peak [15] (see figures 5 and 6). While the Fe3s emission is the preferred mode for addressing magnetic questions, it is obvious from figure 6 that the Fe3p is a much better candidate for the initial geometric-structural studies.

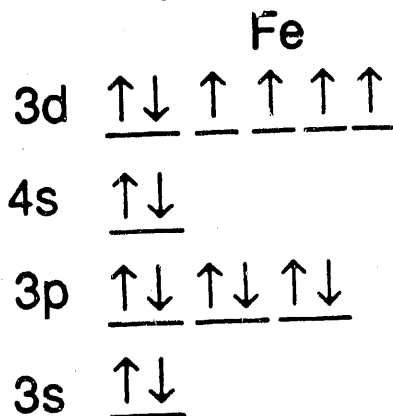
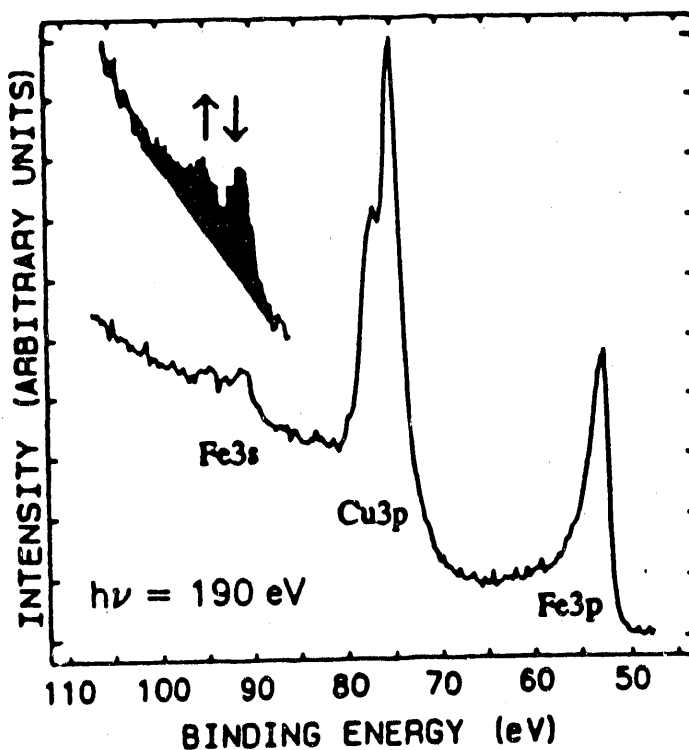


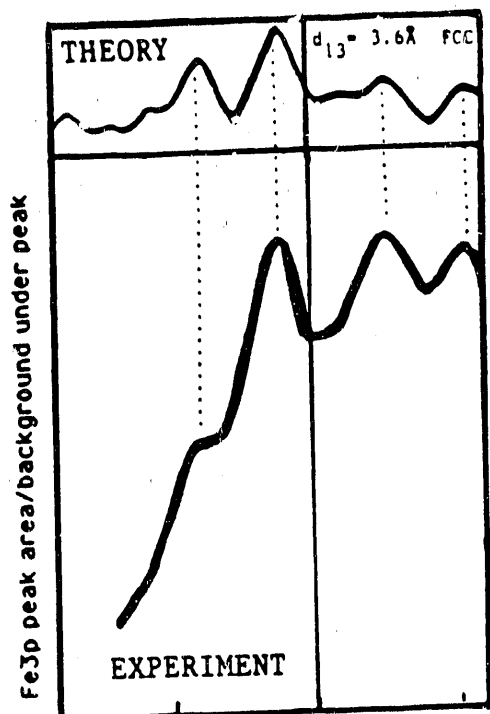
Figure 5. A simplified, atomistic view of the electronic structure of Fe is shown here, to illustrate the cause of the multiplet splitting. If a single 3s electron is removed, the remaining 3s electron will be either parallel or anti-parallel to the aligned 3d electrons. This type of spin-spin interaction affects the overall energetics of the photoemission process, thus producing the splitting in the 3s and the asymmetry in the 3p. This has been confirmed by spin-polarized photoelectron spectroscopy measurements [10, 11, 15].

Figure 6. This figure shows normal emission angle-resolved photo-emission spectra of Fe/Cu(001), using  $h\nu = 190$  eV and with  $\theta = 1^\circ$ . The wide scan shows the Fe3p ( $B^F = 53$  eV), Cu3p ( $B^F = 75, 77$  eV) and the Fe3s ( $B^F = 92$  eV). A narrower scan with better statistics is also shown, which more clearly illustrates the multiplet splitting of the Fe3s peaks. The spin has been assigned to the Fe3s peaks based upon the spin-polarized photoemission results [10, 11].



Preliminary results of the Fe3p photoelectron diffraction experiment suggest that the Fe is in a fourfold hollow site with a spacing between it and the underlying atom (in the third layer) of  $3.6\text{\AA}$  (figure 7). This is consistent with a local FCC structure for the Fe. The calculations were performed using a multiple-scattering slab method and the photo-excitation matrix elements ( $l_i \rightarrow l_{i+1}$ ) are explicitly calculated [16]. The geometric models used include a monolayer, a bilayer and a trilayer of Fe on top of Cu(001), with each successive layer of adsorbates in the fourfold hollow of the previous layer. (See figure 8.) The spacings  $d_{12}$  and  $d_{23}$  were varied independently. The result was that the curves in which  $d_{13} = d_{12} + d_{23} = 3.6\text{\AA}$ , for the monolayer, bilayer and trilayer, were always in fairly good agreement with the experimental curve, regardless of the individual values of  $d_{12}$  and  $d_{23}$ . It is important to remember that while Cu is FCC at higher temperatures and pressures (see figure 3 of ref. 17): Thus, for bulk CuFCC,  $d_{13} = 3.6\text{\AA}$ ; for bulk FeBCC,  $d_{13} = 2.9\text{\AA}$ ; and for FeFCC,  $d_{13} = 3.6\text{\AA}$  (using the data of Table 1 in ref. 17). Hence, it is likely that the Fe is in a FCC site with  $d_{13} = 3.6\text{\AA}$ , but it is not clear whether the Fe is surrounded by Fe, Cu or a mixture of both and whether the intermediate (second) layer is at the expected relaxed FCC position ( $d_{12} = d_{23} = 1.8\text{\AA}$ ). The sensitivity to  $d_{13}$  of the normal emission geometry is the result of the relatively large efficiency of  $180^\circ$  backscattering, as shown in figure 9. To determine  $d_{12}$  and  $d_{23}$  and to lower the error estimate on  $d_{13}$ , it will be necessary for us to extend the data set to other angles (particularly  $45^\circ$ , along the  $[011]$  vectors of Cu(001)) and over a wider kinetic energy range. But to distinguish between Cu and Fe as possible nearest neighbors, it will probably be necessary to resort to spin-dependent photoelectron diffraction. That is because the non-spin scattering factors of Cu and Fe should be very similar, as is born out by the similarity of the monolayer, bilayer and trilayer calculations.

### Fe3p Cross Section vs Kinetic Energy



hv (eV)	150	200	250
KE (eV)	93	143	193

Figure 8. The model used for the multiple scattering calculations is shown here. Calculations were performed using a monolayer, bilayer and trilayer of Fe on top of Cu(001), all assuming epitaxial growth. The spacings between the first and second ( $d_{12}$ ) and second and third layers ( $d_{23}$ ) were systematically varied. The top or first layer was always Fe and the second and third were Fe or Cu, depending upon the model, monolayer, bilayer or trilayer.

Figure 7. The preliminary results of the spin-integrated photoelectron diffraction investigation, using the Fe3p peak, are shown here. The experimental data are shown in a very raw form, in the lower panel. The area of the Fe3p peak is simply divided by the underlying background level, thus normalizing out effects such as photon flux variation. The dropping of the experimental curve with decreasing kinetic energy is caused by the characteristic low kinetic energy tail of secondary electrons, which is commonly observed in photoemission spectra and which can easily be corrected for here [5]. However, it is important that even in this very raw form it is possible to match peak positions with theoretical curves. Shown in the upper panel is the result of a multiple-scattering calculation, with  $d_{13} = 3.6 \text{ \AA}$  and using an epitaxial growth model for a bilayer of Fe on Cu(001). The kinetic energy scale shown here is for  $V_0 = 0$ ; that is, relative to the vacuum zero.

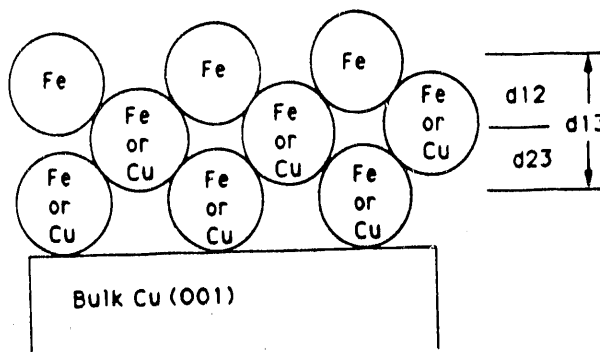
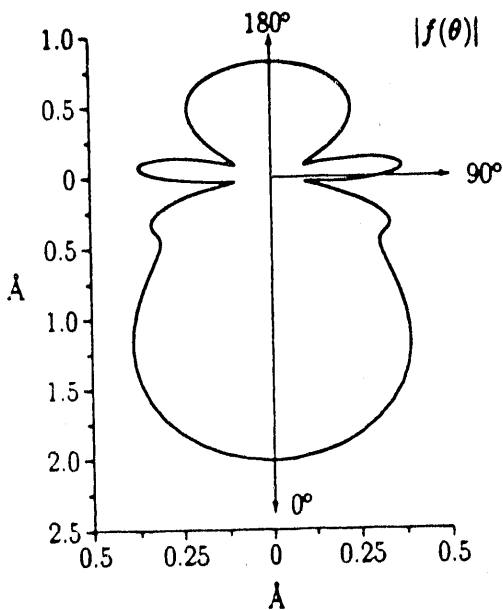


Figure 9. A typical atomic scattering factor of an electron at a kinetic energy of 200eV by a Cu atom is shown here. The fairly large lobe at  $180^\circ$  is the cause of the sensitivity to  $d_{13}$  at normal emission, since it acts to amplify the reflection of the electrons by the underlying atom in the third layer into the detector.



The plausibility of utilizing spin-dependent diffraction with this system is demonstrated by figure 10. Here, it is possible to see the two peak structure at fairly low coverages, without magnetizing the samples. It is of interest that the splitting between the peaks is 3.8eV, in distinct contrast with the bulk value of 4.4eV [18]. Additionally, we have collected data over a narrow range of photon energies ( $230\text{eV} \leq h\nu \leq 260\text{eV}$ ) for a sample with a coverage of  $\Theta = 5/4$ . Obviously, an order of magnitude increase in the data photon energy range is necessary. Nevertheless, if the spin-dependence can be properly incorporated into multiple scattering theory, a probe with nanoscale-magnetic sensitivity may be the result. Moreover, this probe could then be used to follow variations in the local magnetic environment as the sample was macroscopically magnetized.

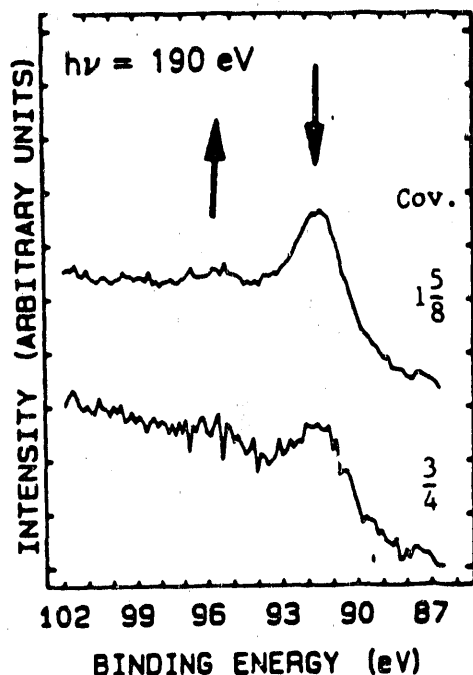


Figure 10. Narrow angle-resolved photoemission spectra of the Fe 3s peaks of Fe/Cu(001) are shown here. The coverages were  $\Theta = 3/4$  (lower) and  $\Theta = 1 5/8$  (upper). The splitting was approximately 3.8eV, significantly different than the bulk value of 4.4eV [18].

#### SUMMARY

Preliminary results of an investigation using photoelectron diffraction to investigate Fe/Cu(001) were presented. Tentatively, the Fe appears to be in a FCC site, with  $d_{13} = 3.6\text{\AA}$ , which is consistent with earlier forward focussing experiments [6,14]. The plausibility of performing spin-dependent photoelectron diffraction on ultrathin magnetic films (sub- and near-monolayer coverages) with the multiplet-split Fe 3s peak was also demonstrated.

#### ACKNOWLEDGEMENTS

Work performed under the auspices of the U.S. Department of Energy by the Lawrence Livermore National Laboratory under contract No. W-7405-ENG-48. S. Y. Tong acknowledges partial support by the Navy under grant no. ONR-00014-90-J-1749. R. Daley of Sandia National Laboratory-Livermore and S. Chaudhuri, who is pursuing a Ph.D. under the direction of R. S. Williams at UCLA, aided in the collection of data at SSRL. H. Gillespie, R. de Souza-Machado and B. Howell performed some of the Auger and LEED experiments.

#### REFERENCES

1. C. L. Fu and A. J. Freeman, Phys. Rev. B **35**, 925 (1987).
2. C. Liu, E. R. Moog and S. D. Bader, Phys. Rev. Lett. **60**, 2422 (1988).
3. J. C. Hansen, M. K. Wagner and J. G. Tobin, Solid State Commun. **72**, 319 (1989); C. M. Wei, J. C. Hansen, M. K. Wagner, R. Machado, R. P. Harvey, J. G. Tobin, and S. Y. Tong, Bril. Am. Phys. Soc. **34**, 446 (1989).
4. B. Sinkovic and C. S. Fadley, Phys. Rev. B **31**, 4665 (1985).



5. J. G. Tobin, L. E. Klebanoff, D. H. Rosenblatt, R. F. Davis, E. Umbach, A. G. Baca, D. A. Shirley, Y. Huang, W. M. Kang and S. Y. Tong, Phys. Rev. B **26**, 7076 (1982). The principle results of this work were subsequently confirmed by SEXAFS measurements: U. Döbler, K. Baberschke, J. Stöhr and D. A. Outka, Phys. Rev. B **31**, 2532 (1985).
6. S. A. Chambers, T. J. Wagener and J. H. Weaver, Phys. Rev. B **36**, 8992 (1987).
7. W. F. Egelhoff, Jr., Phys. Rev. B **30**, 1052 (1984).
8. H. C. Poon and S. Y. Tong, Phys. Rev. B **30**, 6211 (1984).
9. J. G. Tobin, J. C. Hansen and M. W. Wagner, J. Vac. Sci. Technol. A **8**, 2494 (1990).
10. C. Carbone, T. Kachel, R. Rochow and W. Gudat, Z. Phys. B **79**, 325 (1990).
11. F. U. Hillebrecht, R. Jungblut, and E. Kisker, Phys. Rev. Lett. **65**, 2450 (1990).
12. D. P. Pappas, K.-P. Kämper and H. Hopster, Phys. Rev. Lett. **64**, 3179 (1990).
13. D. Pesca, M. Stampanoni, G. L. Bona, A. Vaterlaus, F. Meier, G. Jennings and R. F. Willis, Phys. Rev. Lett. **60**, 2559 (1988).
14. D. A. Steigerwald and W. F. Egelhoff, Jr., Phys. Rev. Lett. **60**, 2558 (1988).
15. C. Carbone and E. Kisker, Solid State Commun. **65**, 1107 (1988).
16. See for example, the review article by S. Y. Tong, Critical Reviews of Solid State Sciences, vol. **10**, 209 (1981), CRC Press; C. H. Li, A. R. Lubinsky and S. Y. Tong, Phys. Rev. B **17**, 3128 (1978).
17. L. N. Falicov, D. T. Pierce, S. D. Bader, R. Gronsky, K. B. Hathaway, H. J. Hopster, D. N. Lambeth, S. S. P. Parkin, G. Prinz, M. Salamon, I. K. Schuller, R. H. Victora, J. Mater. Res. **5**, 1299 (1990).
18. C. S. Fadley, D. A. Shirley, A. J. Freeman, P. S. Bagus and J. V. Mallow, Phys. Rev. Lett. **23**, 1397 (1969).

**END**

**DATE FILMED**

02 / 21 / 91

